

Conserved Quantities and Adapting to the Edge of Chaos in Self-adjusting Dynamical Systems with Wavelet Filtered Feedback

Michael Baym* and Alfred Hübler†

Santa Fe Institute, 1399 Hyde Park Road, New Mexico 87501, USA.

(Dated: April 24, 2005)

Abstract

Certain dynamical systems, such as the shift map and the logistic map, have an edge of chaos in their parameter spaces. On one side of this edge, the dynamics is mostly chaotic, on the other it is periodic. We find that discrete-time dynamical systems with wavelet-filtered feedback from the dynamical variable to the parameters are attracted to narrow parameter range near the edge of chaos, the periodic boundary regime. We show that the migration from the chaotic regime to the periodic boundary regime can be attributed to a conserved quantity, and find that such adaptation to the edge of chaos is accompanied by a depopulation of the chaotic regime. We use this conserved quantity to determine the location of the periodic boundary regime and show that its size is proportional to the size of the feedback. Further, we compute the dynamics of the probability density for the parameter for a specific example.

PACS numbers: 03.30.+p, 03.50.-z, 05.45.-a, 41.60.Bq, 41.75.Jv, 95.30.Jx

*Current address: Department of Mathematics, MIT, 77 Massachusetts Ave., Cambridge, MA 02139

†Permanent address: Center for Complex Systems Research, Department of Physics, 1110 W Green Street, University of Illinois at Urbana-Champaign, Illinois 61801 ; Electronic address: a-hubler@uiuc.edu

I. INTRODUCTION

The concept "adaptation to the edge-of-chaos" refers to the idea that many complex adaptive systems, including those found in biology, seem to naturally evolve towards a narrow regime near the boundary between order and chaos[1]. Packard [2] first showed that this effect occurs for a population of cellular automata rules evolving with a genetic algorithm, though the conclusions drawn from this work have come under some dispute [3]. Self-organized criticality [4] in avalanche and earthquake models is believed to be a related phenomenon. Models of coupled neurons with self-adjusting coupling strength have been found to exhibit robust synchronization and suppression of chaos [5]. The edge of chaos occupies a prominent position because it has been found to be not only the optimal setting for control of a system [6], but also an optimal setting under which a physical system can support primitive functions for computation[7], though once again this claim has been disputed[8]. Possibly the simplest models for adaptation to the edge of chaos are self-adjusting map dynamics [9]. The numerical findings have been confirmed experimentally[10] with Chua's circuit[11]. However, the theoretical analysis does not predict the location of the narrow parameter regime near the boundary to which the system evolves. Furthermore the distribution function for the limiting parameter values differ from numerical findings. This is believed to be due to the fact that the dynamics of the parameters is approximated by a diffusion process with a large diffusion constant in the chaotic regime. In Melby's system, the feedback from the dynamical variable to the map parameter is computed with a windowed Fourier band filter. This is a rather complicated algorithm whereas wavelet filters [12, 13] have a similar effect, but are much simpler in both implementation[14–16] and analysis. Wavelet filters have been successfully used for the compression of experimental data [17–24] as well as images in JPEG format [25]. Finitely supported wavelet filters can be good models for the dynamics of slow variables in naturally occurring processes [26, 27].

In this paper, we study the evolution of self-adjusting maps towards the edge of chaos. In contrast to earlier work, we assume that the feedback from the dynamical variable is low-pass wavelet-filtered. We use discrete wavelet filters that have a finite support and have zero mean. Further we consider the impact of correlations in the parameter dynamics and determine the location of the narrow regime near the edge of chaos to which the dynamics evolve. Finally we determine the dynamics of the probability density of the parameter for a

specific example.

II. SELF-ADJUSTING MAP DYNAMICS

We consider a self-adjusting map dynamics with the dynamical variable x_n on the interval and a self-adjusting parameter a_n :

$$\begin{aligned} x_{n+1} &= f(x_n, a_n) \\ a_{n+1} &= a_n + s_n \Delta F_n \end{aligned} \tag{1}$$

where the wavelet filter $\Delta F_n = \sum_{i=0}^{M-1} g_i x_{n+1-i}$ with finite support M and zero mean. For Daubechies wavelets of order one with support $M=4$ the wavelet coefficients are $g_0 = (1 - \sqrt{3})/\sqrt{2}$, $g_1 = -(3 - \sqrt{3})/\sqrt{2}$, $g_2 = (3 + \sqrt{3})/\sqrt{2}$, and $g_3 = -(1 + \sqrt{3})/\sqrt{2}$ [13]. For a Haar wavelet the coefficients are $g_0 = -g_1 = 1$. During the adaption periods the size of the feedback is small and constant, i.e. $0 < s_n = s \ll 1$ at the time step $n = iN, iN + 1, \dots, (i+1)N - 1$, $i = 1, 3, \dots$. During the relaxation periods, $n = iN, iN + 1, \dots, (i+1)N - 1$, $i = 0, 2, \dots, I$ there is no feedback, i.e. $s_n = 0$. For systems with a bounded parameter range, $a_{min} \leq a_n \leq a_{max}$, the parameter is set equal to the boundary value if the new value would be outside the parameter range, i.e. $a_{n+1} = a_{max}$ if $a_n + s_n \Delta F_n > a_{max}$ and $a_{n+1} = a_{min}$ if $a_n + s_n \Delta F_n < a_{min}$. Further we assume that the adaption and relaxation periods are long compared to the support of the filter, i.e. $N \gg M$, and long compared to the relaxation time of the dynamical system x_{jN} , $j = 1, 2, \dots$, so that it can reach the vicinity of an attractor before adaption is turned on or off again. The initial state x_0 is assumed to be random and equally distributed.

Fig. 1 shows typical numerical results generated from Eq. (1) for the shift map $f = \text{mod}(a_n x_n + r_n)$, where $-5 \times 10^{-6} < r_n < 5 \times 10^{-6}$ are random and equally distributed and $0 \leq a_n \leq 2$. The modulo function is defined as $\text{mod}(x) = x - \text{int}(x)$, where $\text{int}(x)$ returns the integer portion of x . If the initial parameter value is in the chaotic regime, i.e. $a_n > 1$ the parameter value is changing within a certain range during the adaptation periods. Even though a_n stays within a small range during each adaptation period, these

ranges are different at each adaptation period and eventually the parameter value reaches the period regime $a_n < 1$ and stays there.

The *total wavelet filter* is defined as

$$F_n := \sum_{i=0}^{M-2} w_i x_{n+1-i} \quad (2)$$

where $w_i = \sum_{j=0}^i g_j$ (**NEW** are the coefficients of the *integrated wavelet* . Hence $F_{n+1} - F_n = \Delta F_n$ and $F_n = F_{n_0} + \sum_{i=n_0}^n \Delta F_i$ if $n_0 \leq n$. **NEW**) In contrast to the parameter a_n , the quantity b_n defined as:

$$b_n = a_n - s_n F_n \quad (3)$$

is conserved, i.e. $b_{n+1} = a_{n+1} - s_{n+1} F_{n+1} = (a_n + s_n F_{n+1} - s_n F_n) - s_{n+1} F_{n+1} = (a_n - s_n F_n) - (s_{n+1} - s_n) F_{n+1} = a_n - s F_n = b_n$, except when $s_{n+1} \neq s_n$ at the time steps when the adaptation is switched on or off.

In addition, if a_n reaches the boundary of the parameter range during the adaption period, b_n is not constant. Then $b_n = b_{iN} + \sum_{m=iN}^{n-1} (a_{m+1} - a_m - s_m \Delta F_m)$. (**COM** If $a_{n+1} = a_n + s_n \Delta F_n + \Delta a_n$ where Δa_n is the correction when $\Delta a_a = a_{max} - (a_n + s_n \Delta F_n)$ if $a_n + s_n \Delta F_n > a_{max}$ and $\Delta a_a = 0$ else. Then $b_{n+1} = a_{n+1} - s_{n+1} F_{n+1} = (a_n + s_n F_{n+1} - s_n F_n + \Delta a_n) - s_{n+1} F_{n+1} = (a_n - s_n F_n) - (s_{n+1} - s_n) F_{n+1} + \Delta a_n = a_n - s F_n + \Delta a_n = b_n + \Delta a_n$. Hence $b_n = b_{iN} + \sum_{m=iN}^{n-1} \Delta a_m = b_{iN} + \sum_{m=iN}^{n-1} (a_{m+1} - a_m - s_m \Delta F_m)$. **COM**) Fig. 2 shows the time dependence of b_n for the dynamics in Fig. 1.

We can use the conserved quantity to eliminate the dynamical variable a_n from Eq. (1):

$$x_{n+1} = g(x_n, \dots, x_{n-M+1}, s_n, b_{iN}) \quad (4)$$

where $g(x_n, \dots, x_{n-M+1}, s, b_{iN}) = f(x_n, b_{iN} + s F_n)$ and $F_n = F(x_n, \dots, x_{n-M+1})$. While the conserved quantity is constant during the adaptation periods and the relaxation periods, it may change whenever the adaptation is switched on or off.

From Eq. 1 and Eq. ?? we conclude (**COM** Given: $F_{n+1} - F_n = \Delta F_n$, $b_n = a_n - s_n F_n$, $a_{n+1} = a_n + s_n \Delta F_n$. For i even, $\dots, s_{iN-2} = s$, $s_{iN-1} = s$, $s_{iN} = 0$, $s_{iN+1} = 0$, \dots . Hence $b_{iN} = a_{iN} = a_{iN-1} + s \Delta F_{iN-1} = a_{iN-1} + s F_{iN} - s F_{iN-1} = b_{iN-1} + s F_{iN}$. For i odd, $\dots, s_{iN-2} = 0$, $s_{iN-1} = 0$, $s_{iN} = s$, $s_{iN+1} = s$, \dots . Hence $b_{iN} = a_{iN} - s F_{iN} =$

$a_{iN-1} - sF_{iN} = b_{iN-1} - sF_{iN}$. **COM**) that the dynamics of b_n , as illustrated in Fig. 2, is governed by the mapping function

$$b_n = \begin{cases} b_{n-1} + (-1)^i s F_{iN} & \text{if } n = iN, i \in \mathbb{N} \\ b_{n-1} & \text{otherwise} \end{cases} \quad (5)$$

where F_{iN} is the value of the filter function at the end of a relaxation period, for $i = 0, 2, \dots$ and otherwise a value of filter function at the end of an adaptation period. Since we assume that the adaptation and relaxation periods are long enough for the system to reach its attractors, the range of the values of the filter function F_{iN} at the end of each periods depends only on the value of the conserved quantity b , and the size of the feedback s . Hence for $i = 0, 2, \dots$ we find $F_{iN} \in [F_{min}(b_{iN}, s), F_{max}(b_{iN}, s)]$ and otherwise $F_{iN} \in [F_{min}(b_{iN}, 0), F_{max}(b_{iN}, 0)]$. Whenever adaptation is switched on or off, the conserved quantity changes by a small amount of order s

$$\begin{aligned} b_{iN} - sF_{max}(b_{iN}, s) \leq b_{(i+1)N} \leq b_{iN} - sF_{min}(b_{iN}, s) & \text{ if } i = 0, 2, \dots \\ b_{iN} + sF_{min}(b_{iN}, 0) \leq b_{(i+1)N} \leq b_{iN} + sF_{max}(b_{iN}, 0) & \text{ else} \end{aligned} \quad (6)$$

Since b_n is conserved during adaptation periods (see Eq. (??)), a_n stays within a small range of order s

$$b_{iN} + sF_{min}(b_{iN}, s) < a_n < b_{iN} + sF_{max}(b_{iN}, s) \quad (7)$$

where $iN \leq n < (i+1)N$ and $i = 1, 3, \dots$ (see Fig. 1).

In the following, we assume that for $s = 0$ the parameter a of the map dynamics has an edge of chaos at a_c , i.e. there exists a band of width $\epsilon > 0$ about a_c such that when $a_c - \epsilon < a_n < a_c$, there exists only periodic attractors with periods $k < k_c$, and when $a_c < a_n < a_c + \epsilon$ the dynamics are chaotic.

Since wavelet filters act as sub-band filters [13], i.e. low-frequency band filters with cut-off period k_c , they can detect the edge of chaos. The filter output ΔF_n is very small or zero for periodic time series with a recurrence time below k_c , whereas for chaotic time series ΔF_n is irregular. The edge of chaos a_c as detected by the wavelet filter depends on a threshold ΔF_t , i.e. $\max |\Delta F(a_n)| = \Delta F_t$ for $a_n = a_c$ and $\max |\Delta F(a_n)| < \Delta F_t$ for $a_n < a_c$. Fig. 3 shows the edge of chaos a_c for a family of wavelets, including the Haar wavelet), as a function of

the length of the support M . For the shift map and the logistic map wavelets can detect the edge of chaos with high precision even if their support is small.

Hence, we assume that the limiting value of ΔF is zero, i.e. $\Delta F = 0$ for $a_n < a_c$ and $s = 0$. Fig. 4 shows the self-adjustment ΔF_n versus a_n for a shift map where $a_c = 1$. From Eq. 1 we conclude that if the parameter value below the edge of chaos during a relaxation period, then the self-adjustment is zero from then on, hence for all $n \geq iN$

$$\Delta F_n = 0 \text{ if } a_{iN} < a_c \quad (8)$$

and if $i \in \{0, 2, \dots\}$. To investigate the statistical properties of the system, we study a large ensemble where the initial parameter values are homogeneously distributed in the interval $I = [a_{min}, a_{max}]$. $P_n(b)$ is probability density of the b_n -values at time n , hence $P_0 = 1/(a_{max} - a_{min})$. Since $a_n = b_n$ during the relaxation periods, the probability density of the a_n -values equals the probability density of the b_n -values, i.e. the probability density of the a_n values is $P_n(a)$. Next we discuss the change of the b_n -values from relaxation period to relaxation period and how this affects P_n . If the parameter value is below the edge of chaos it is constant even during adaptation periods (see Eq. 8). Hence, in the period regime the probability density of the parameter P_n stays same or increases at the expense of the probability density in the chaotic regime,

$$P_{(i+2)N} \geq P_{iN} \text{ if } b < a_c \quad (9)$$

for $i = 0, 2, \dots$. In the following we show that growth of the probability density occurs mostly in the boundary of the periodic regime. Since the b_n changes only by a small amount given by Eq. (4) whenever adaptation is switch on or off, and otherwise b_n is constant, only parameter values in the vicinity of the edge of chaos can reach the periodic regime during one adaptation period. Systems with parameters further away from the edge of chaos can reach the periodic regime, only after adaptation has been repeatedly switched on and off.

Systems with $b_{iN} > a_c$ during the relaxation period, may have a parameter value below a_c during the adaptation period. Fig. 5 shows typical b -values during the adaptation period values as a function of the a -value during the relaxation period for a shift map. If $F_{max}(b, 0)$ doesn't increase rapidly at the edge of chaos, i.e. $(F_{max}(b, 0) - F_{max}(a_c, 0))/(b - a_c) < 1$ then the minimum b -value is $b_{min} = a_c - sF_{max}(a_c, 0)$. If $F_{min}(b_{min}, s)$ doesn't decrease rapidly

at the b_{min} , i.e. $(F_{min}(b, s) - F_{min}(b_{min}, s))/(b - b_{min}) > -1$ then we conclude from Eq. (6) that the probability density of the b -values increases in the periodic boundary region and remains constant in the remainder of the periodic regime

$$P_{(i+2)N} \begin{cases} > P_{iN} & \text{if } a_b \leq b \leq a_c \\ = P_{iN} & \text{if } b < a_b. \end{cases} \quad (10)$$

for $i = 0, 2, \dots$, where $a_b = a_c - sF_{max}(a_c, 0) + sF_{min}(a_c - sF_{max}(a_c, 0), s)$. The periodic boundary region, $a_b \leq b \leq a_c$ is just below a_c . If we approximate $F_{min}(b_{min}, s) \approx F_{min}(b_{min}, 0) + s * \frac{d}{ds}F_{min}(b_{min}, 0) + O(s^2)$, we obtain for the lower bound of the periodic boundary region

$$a_b = a_c - s(F_{max}(a_c, 0) - F_{min}(b_{min}, 0)) - s^2 \frac{d}{ds}F_{min}(b_{min}, 0) \quad (11)$$

Fig. 6 illustrates the periodic boundary regime for a self-adjusting logistic map dynamics and the parameter range where the class frequencies increase. For the self-adjusting logistic map we find numerically $F_{max}(a_c, 0) \approx F_{min}(b_{min}, 0)$ and $\frac{d}{ds}F_{min}(b_{min}, 0) \approx 0.036$ for $M = 2$. The increase of the probability density in the periodic boundary region is at the expense of the probability density in the chaotic regime. The migration of the population from the chaotic regime to the periodic boundary region is a concrete model for *adaptation to the edge of chaos*. The population in the chaotic regime evolves towards a narrow regime near the boundary between order and chaos.

In the following we compute dynamics of the probability density of the parameter values p_n and the dynamics of the probability density of the x -values ρ_n for a specific example, a self-adjusting shift map $x_{n+1} = \text{mod}(a_n * x_n + r_n)$ with a Haar wavelet filter, where $a_{min} = 0$, $a_{max} = 2$ and r_n is small band limited white noise, $-10^{-7} < r_n < 10^{-7}$. For the self-adjusting shift map, the edge of chaos is $a_c = 1$ and $F_{max}(a_c, 0) = 1$ and $F_{min}(b_{min}, 0) = 0$. Therefore the periodic boundary region is $1 - s < b < 1$.

If $0 \leq b_{iN} \leq 1$, the dynamics has a fixed point at $x_n = 0$, and the limiting probability density of the x_{iN} values for $s = 0$ is $\rho_{iN} = \delta(x)$, where δ is the Kronecker's δ -function. If $b_{iN} \geq 1$, the dynamics the dynamics is chaotic. For small s , i.e. $0 \leq s \leq 0.3$ and b_{iN} -values close to unity, i.e. $1 \leq b_{iN} \leq 1.5$, the limiting probability density of the x -values can be approximated by

$$\rho_{iN}(x) = \begin{cases} d/(b_{iN} - a_c) & \text{if } 0 \leq x < b_{iN} - a_c \\ d/x & \text{if } b_{iN} - a_c \leq x \leq 1 \\ 0 & \text{else} \end{cases} \quad (12)$$

where $d = 1/(1 - \ln(b - a_c)) = \alpha + \beta b + O^2(a_c + 0.25 - b)$, for $a_c = 1$ where $\alpha = (2 \ln 2 - 4)/(1 + 2 \ln 2)^2$, and $\beta = 4/(1 + 2 \ln 2)^2$. Fig. 7 shows a comparison between a histogram of the numerical class frequencies and analytical results in Eq. 12.

Since $b_{(i+1)N} = b_{iN} - sF_{(i+1)N} = b_{iN} - sx_{(i+1)N}$, the conditional probability $T(b|a)$ that the conserved quantity has the value b during an adaptation period, given that it is the value a during the preceding relaxation period is $T(b|a) = \rho_{(i+1)N}((a - b)/s)$ for $i = 0, 2, \dots$. Hence

$$T(b|a) = \begin{cases} \delta(a - b) & \text{if } a \leq a_c \\ \frac{d}{s(a - a_c)}, & \text{if } 0 \leq \frac{a - b}{s} \leq a - a_c \\ \frac{d}{a - b}, & \text{if } a - a_c \leq \frac{a - b}{s} \leq 1 \\ 0 & \text{else} \end{cases} \quad (13)$$

Fig. 8 shows the conditional probability $T(b|a)$ and the corresponding class frequencies for $a = 1.1$. The probability of the conserved quantity $p_{(i+1)N}(b) = \int_{a_{min}}^{a_{max}} T(b|a)p_{iN}(a)da$. For $b < a_c$ this integral simplifies to $p_{(i+1)N}(b) = 1 + \int_{a_c}^{b+s} T(b|a)p_{iN}(a)da$. For the first few adaptation/relaxation cycles we can assume that the probability density in the chaotic regime near the edge of chaos is roughly constant $p(a) = 1$ for $a_c < a < a_c + s$. Then $p_{(i+1)N}(b) = 1 + \int_{a_c}^{b+s} T(b|a)da = 1 + \int_{a_c}^{b+s} \frac{d}{a - b} da$. Hence for first couple of adaptation/relaxation cycles $i = 0, 2, \dots, 2(a_{max} - b_c)/s$, the probability of the conserved quantity is approximately

$$p_{(i+1)N}(b) = \begin{cases} 1 & \text{if } a_{min} \leq b \leq a_c - s \\ (\beta(b + s - b_c) + (\beta b + \alpha) \ln \frac{s}{a_c - b}) \frac{i}{2} + 1 & \text{if } a_c - s < b < a_c \\ 1 & \text{if } a_c \leq b \leq a_{max} - \frac{is}{2} \\ 1 - C/s & \text{if } a_{max} - \frac{is}{2} \leq b \leq a_{max} \end{cases} \quad (14)$$

where $C = \int_{a_c - s}^{a_c} (\beta(b + s - b_c) + (\beta b + \alpha) \ln \frac{s}{a_c - b}) db \approx (\beta + \alpha)s + \frac{\beta}{4}s^2$. During the relaxation periods the probabilities for classes in the periodic regime is the same as during the first adaptation period, $P_{a,2N}a_k = P_{b,2N}a_k$ if $a_k < a_c$. Fig. 9 shows the class frequencies for the b -values and the limiting probabilities computed with Eq. (14).

After many cycles the population reaches a limiting distribution

$$p(b) = \begin{cases} 1 & \text{if } a_{min} \leq b \leq a_c - s \\ (\beta(b + s - a_c) + (\beta b + \alpha) \ln \frac{s}{a_c - b})/C + 1 & \text{if } b_c - s < b_k < b_c \\ 0 & \text{if } a_c \leq b \leq a_{max} \end{cases} \quad (15)$$

Eq. and indicate that the population in the periodic boundary region is increasing at each adaption/relaxation cycle, until the chaotic regime is depopulated. Fig. 10 shows the limiting class frequencies for the b-values and the limiting probabilities computed with Eq. (15).

-
- [1] S. A. Kauffman, *The origins of order: Self-organization and selection in evolution* (Oxford University Press, New York, 1993).
- [2] N. H. Packard, in *Dynamic patterns in complex systems*, edited by J. A. S. Kelso, A. J. Mandell, and M. F. Schlesinger (World Scientific, Singapur, 1988), pp. 293–301.
- [3] M. Mitchell, P. T. Hraber, and J. P. Crutchfield, *Complex Systems* **7**, 89 (1993).
- [4] P. Bak, C. Tang, and K. Wiesenfeld, *Phys. Rev. A* **38**, 364 (1988).
- [5] V. P. Zhigulin, M. I. Rabinovich, R. Huerta, and H. D. I. Abarbanel, *Phys. Rev. E* **67**, 021901 (2003).
- [6] D. Pierre and A. Hubler, *Physica* **75D**, 343 (1994).
- [7] C. A. Langton, *Physica* **42D**, 12 (1990).
- [8] A. Adamatzky and O. Holland, *Chaos, Solitons and Fractals* **9**, 1233 (1998).
- [9] P. Melby, J. Kaidel, N. Weber, and A. Hubler, *Phys. Rev. Lett.* **84**, 5991 (2000).
- [10] P. Melby, N. Weber, and A. Hubler, *Fluct. Noise Lett.* **2**, L285 (2002).
- [11] L. O. Chua, T. Matsumoto, and M. Komuro, *IEEE Trans. on Circuits and Systems* **cas-33** (1986).
- [12] I. Daubechies, *Ten Lectures on Wavelets*, no. 61 in CBMS-NSF Series in Applied Mathematics (Society for Industrial and Applied Math., Philadelphia, 1992).
- [13] A. Jense and A. la Cour-Harbo, eds., *Ripples in Mathematics: the Discrete Wavelet Transform, Wavelet Analysis and Its Applications* (Springer, New York, 2001).
- [14] G. Beylkin, R. Coifman, and V. Rokhlin, *Comm. in Pure and Applied Math.* **44**, 141 (1991).
- [15] A. H. Tewfik, D. Sinha, and P. Jorgensen, *IEEE Trans. Inf. Theory* **38**, 747 (1992).
- [16] D. F. Walnut, *An Introduction to Wavelet Analysis*, Applied and Numerical Harmonic Analysis (Birkhauser, Boston, 2003).
- [17] A. Arneodo, G. Grasseau, and M. Holschneider, *Phys. Rev. Lett.* **61**, 2281 (1988).
- [18] F. Argoul, A. Arneodo, J. ELezgaray, G. Grasseau, and R. Murenzi, *Phys. Rev. Lett. A* **135**, 327 (1988).
- [19] F. Argoul, A. Arneodo, J. ELezgaray, G. Grasseau, and R. Murenzi, *Phys. Rev. A* **41**, 5537 (1988).
- [20] F. Argoul, A. Arneodo, G. Grasseau, Y. Gagne, E. J. Hopfinger, and U. Frisch, *Nature* **338**,

51 (1989).

- [21] J. F. Muzy, E. Barcy, and A. Arneodo, *Phys. Rev. Lett.* **67**, 3515 (1991).
- [22] M. Yamada and K. Ohkitani, *Prog. Theor. Phys.* **86**, 799 (1991).
- [23] B. J. Turner and M. Y. LeClerc, *J. Atmospheric and Oceanic Techn.* **11**, 205 (1994).
- [24] T. Dallard and F. K. Browand, *J. Fluid Mech.* **247**, 339 (1993).
- [25] D. Mackenzie, *Wavelets: Seeing the forest - and the trees*, Beyond Discovery (National Academy of Sciences, Washington, 2001).
- [26] M. Vergassola and U. Frisch, *Physica D* **54**, 58 (1991).
- [27] S. Qian and J. Weiss, *J. Comp. Phys.* **106**, 155 (1993).

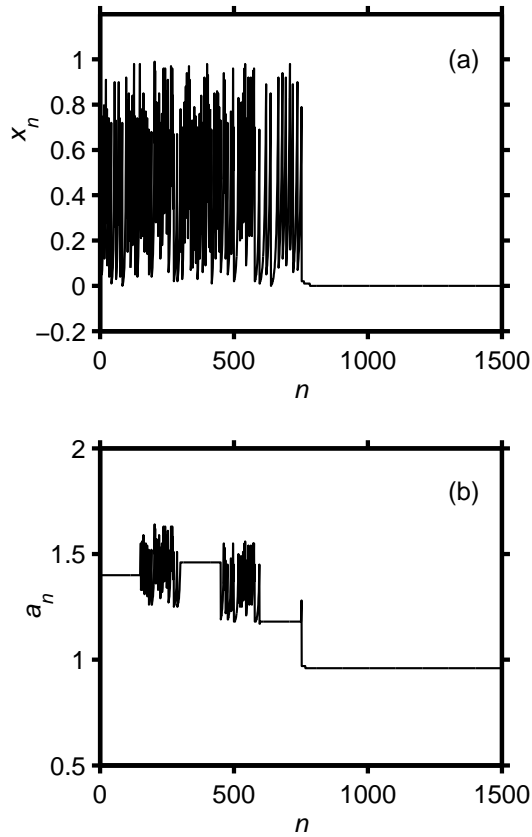


FIG. 1: The value of the dynamical variable x_n versus time step n (a) and the value of the parameter a_n versus time step n (b) for a shift map, where $s = 0.4$, $N = 150$ and a Haar wavelet filter. a_n is constant if the self-adjustment is off. If the self-adjustment is on and a_n is in the chaotic regime $a_n > 1$, the parameter value has an irregular time dependence, but stays within a small range. In this simulation the parameter value a_n , never reaches the boundaries of the parameter range $a_{min} = 0$ and $a_{max} = 2$.

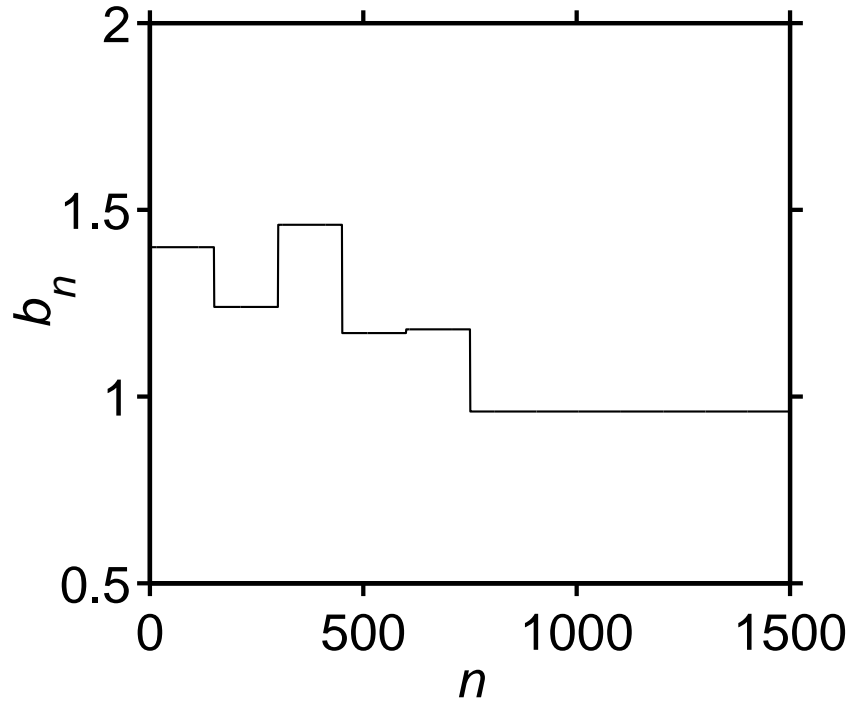


FIG. 2: The value of $b_n = a_n - sF_n$ versus time step n . This plot illustrates that b_n is a conserved except when the self-adjustment is switched on/off.

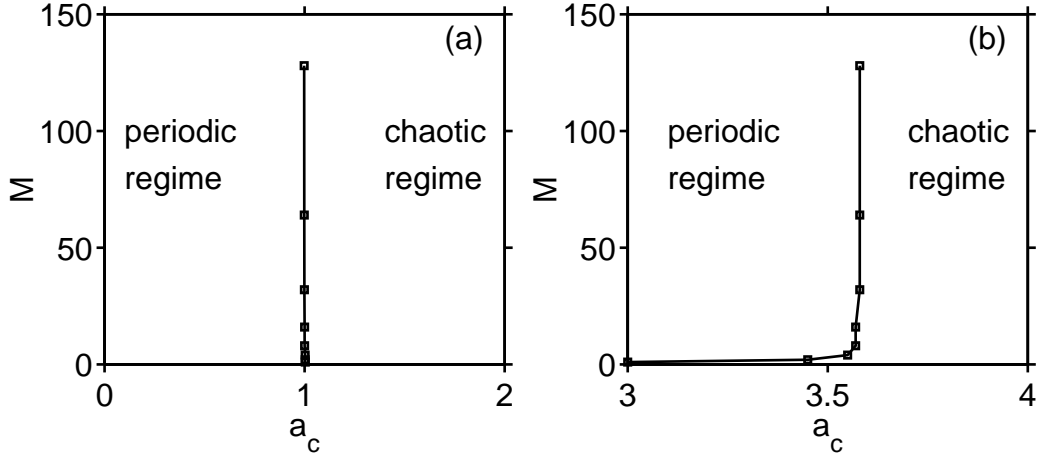


FIG. 3: The edge of chaos a_c as detected by a wavelet filter as a function of length of the support M , for the shift map $x_{n+1} = \text{mod}(a_n x_n + r_n)$ (a) and a logistic map $x_{n+1} = a_n x_n (1 - x_n)$ (b). The wavelet coefficients are $g_0 = 1$, $g_{M-1} = -1$ and $g_i = 0$ for $i = 1, 2, \dots, M - 2$. The threshold is $\Delta F_t = 0.002$. The theoretical values are $a_c = 3.57$ for the logistic map and $a_c = 1$ for the shift map.

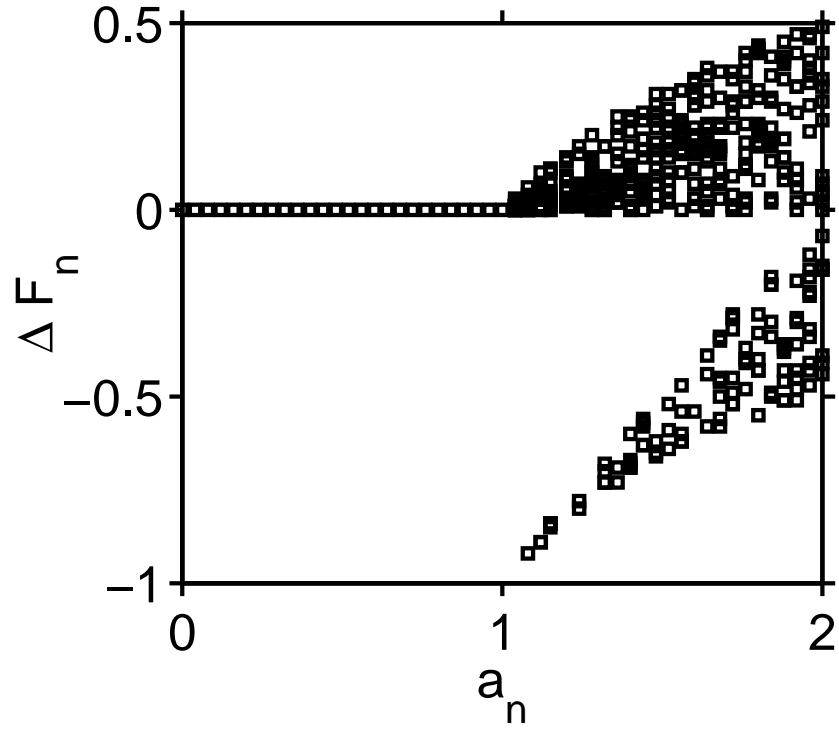


FIG. 4: Typical ΔF_n -values versus the value for the parameter a for a shift map with a Haar wavelet filter. This plot illustrates that $\Delta F_n = 0$ if $a_n < a_c$, where $a_c = 1$.

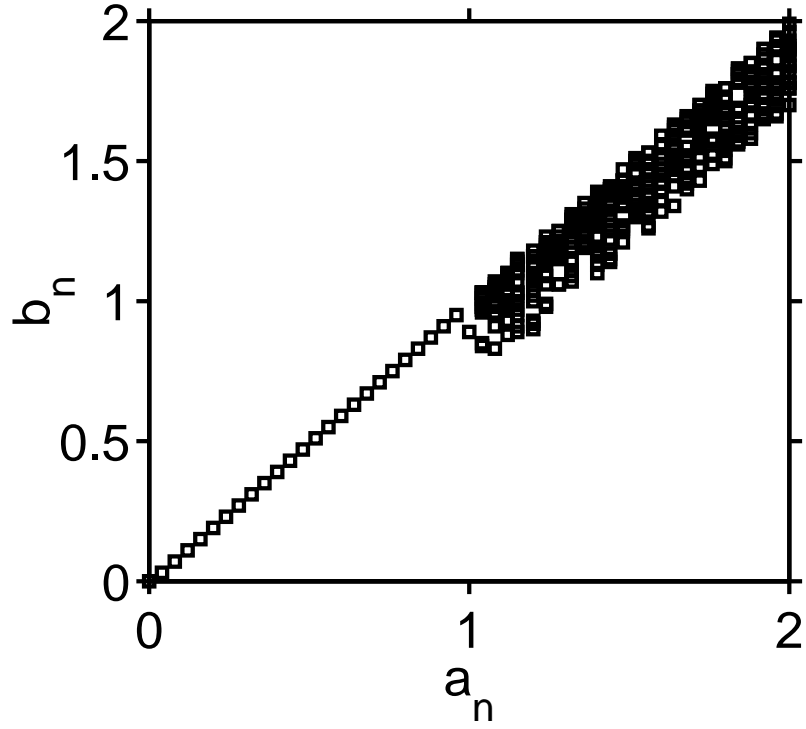


FIG. 5: Typical b -values during the adaptation period versus the value for the parameter a during the preceding relaxation period for a shift map with a Haar wavelet filter and $s = 0.3$. This plot illustrates that $b_n = a_n$ if $a_n < a_c$, where $a_c = 1$.

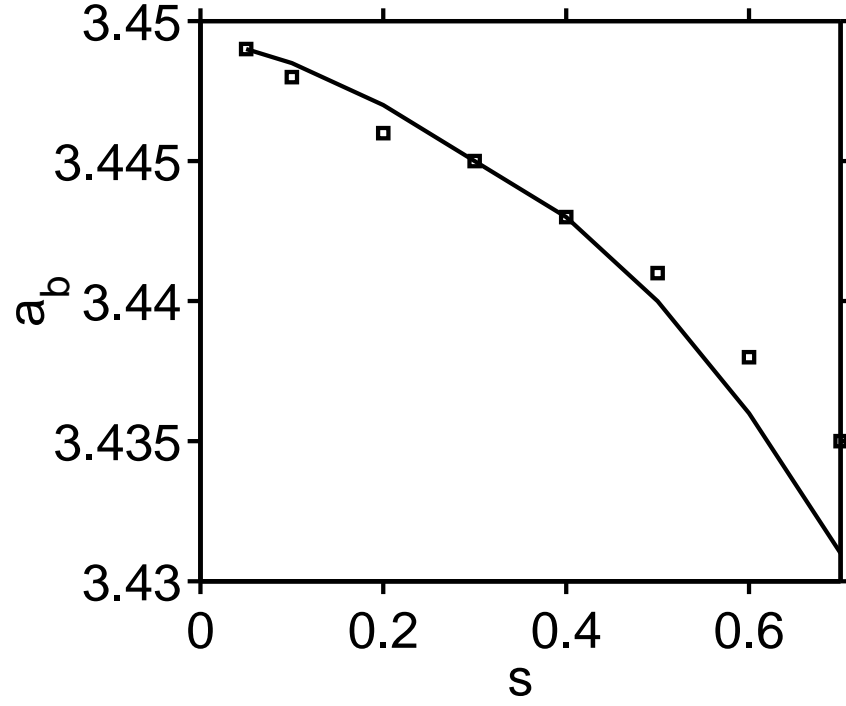


FIG. 6: The lower bound of the periodic boundary regime a_b . The squares indicate numerical values, the continuous lines defined by Eq. (11) for a logistic map $x_{n+1} = a_n x_n (1 - x_n)$ with a Haar wavelet filter, where $a_c = 3.449$. The probability density increases in the interval $a_b < a < a_c$.

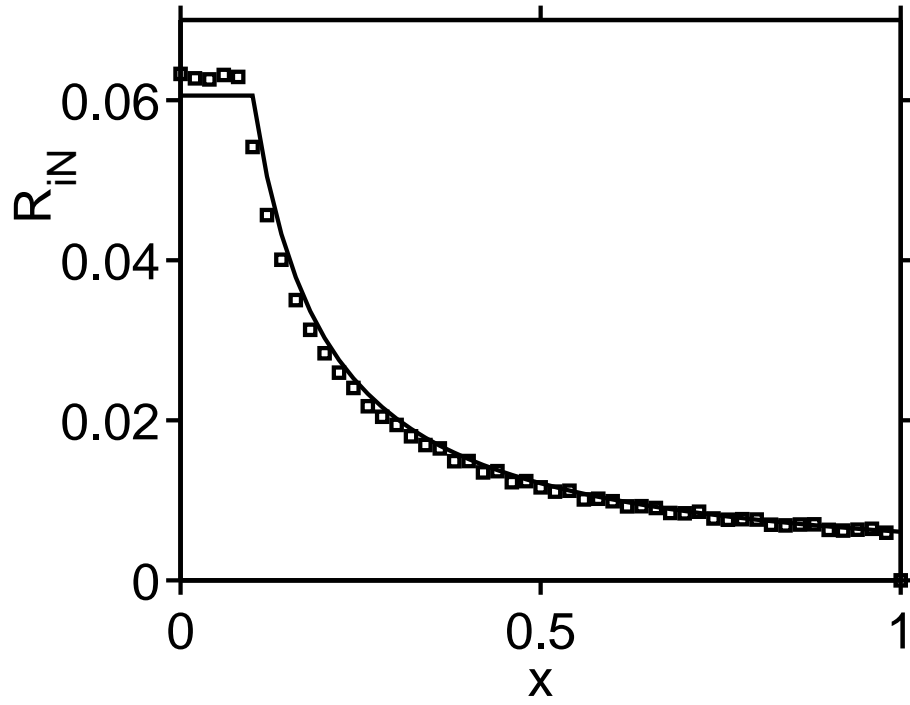


FIG. 7: $R_{x,iN}(x_r) = \rho_{x,iN}(x_r) * \Delta x$, the probability of the x_n values in a bin of size $\Delta x = 0.04$ of a self-adjusting shift map with a Haar wavelet filter and $s = 0.3$. The squares are a histogram of the numerical values of relative class frequencies of the x -values determined numerically where the sample size is $N = 10^6$.

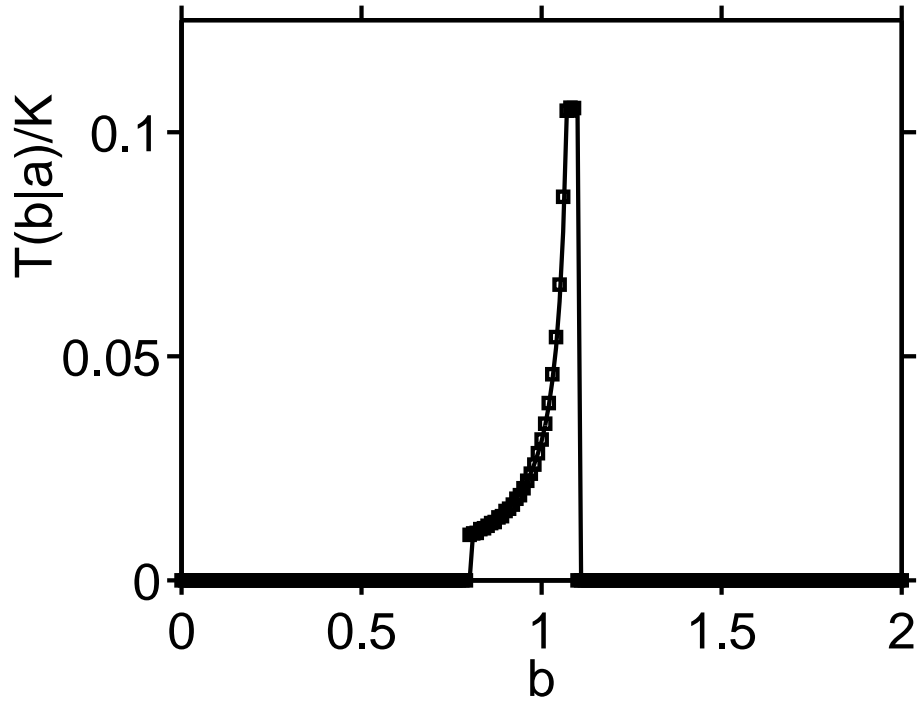


FIG. 8: shows the conditional transition probability $T(b|a)/K$ of the conserved quantity at the beginning of the adaptation period and the corresponding numerical class frequencies (squares) for $a = 1.1$, sample size $N = 10^6$, $s = 0.3$, and $K = 200$ classes.

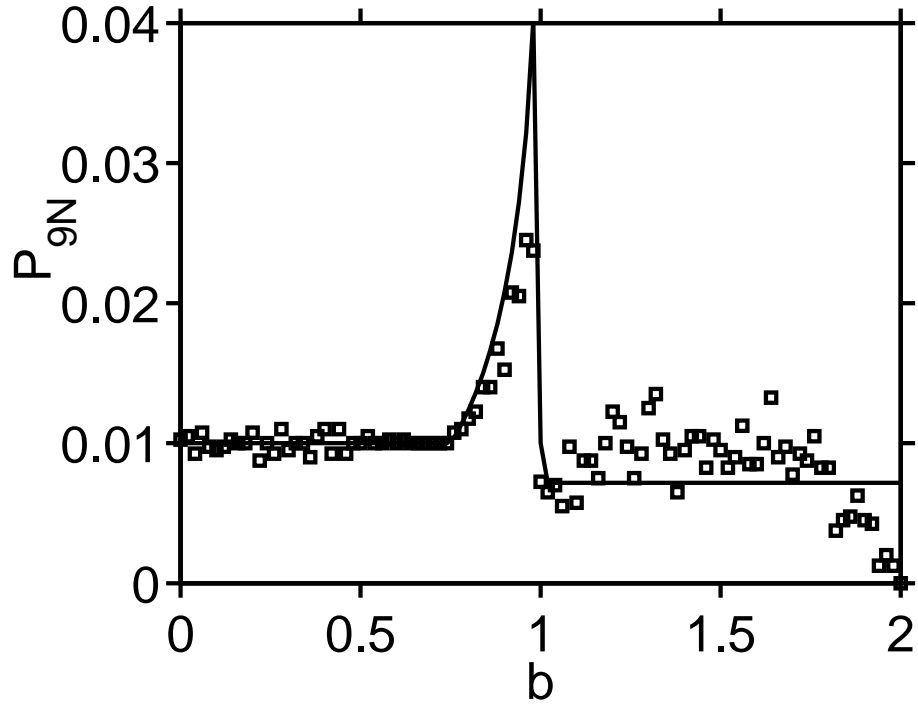


FIG. 9: The numerical values of the relative class frequencies (squares) and the probabilities of the b -values $P_{9N} = p_{9N}/K$ of a self-adjusting shift map with a Haar wavelet filter for $s = 0.25$, $N = 500$, and $K = 100$.

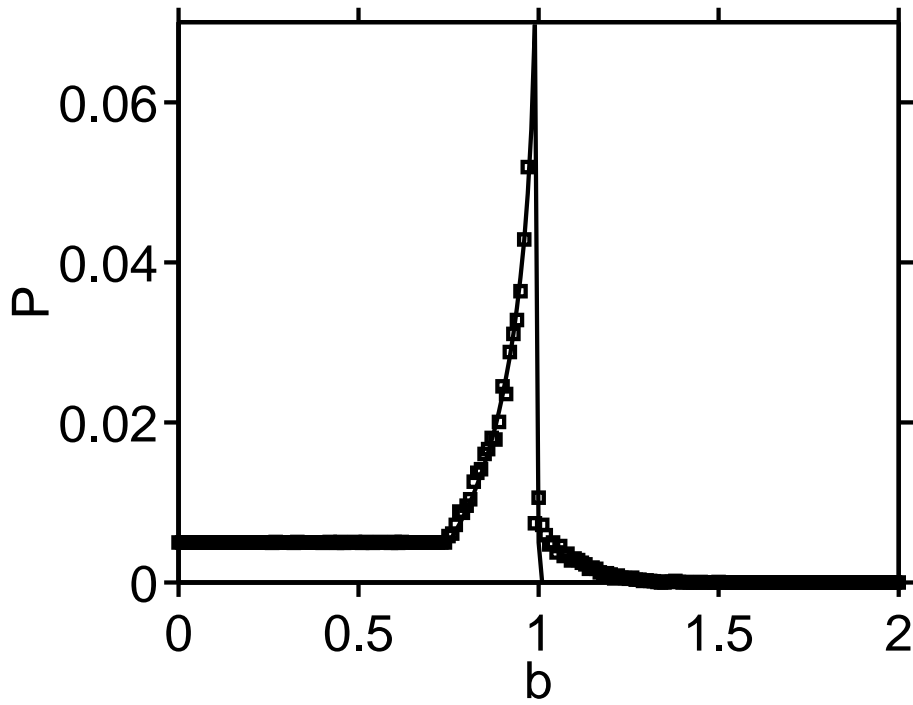


FIG. 10: The numerical values of the limiting relative class frequency (squares) and the limiting probability $P(b) = p(b)/K$ of the b -values of a self-adjusting shift map with a Haar wavelet filter, $s = 0.25$, $N = 500$, and $K = 200$.